Decoding resistance to immune checkpoint inhibitors in non-small cell lung cancer: a comprehensive analysis of plasma proteomics and therapeutic implications

Michal Harel [1], Nili Dahan,[1] Coren Lahav [1], Eyal Jacob,[1] Yehonatan Elon,[1] Igor Puzanov [2,3] Ronan J Kelly,[4] Yuval Shaked [5], Raya Leibowitz,[6] David P Carbone [7], David R Gandara [8] Adam P Dicker[9]

For numbered affiliations see end of article.

Correspondence to
Dr Michal Harel;
michal@oncohost.com

ABSTRACT

Background Immune checkpoint inhibitors (ICIs) have shown substantial benefit for patients with advanced non-small cell lung cancer (NSCLC). However, resistance to ICIs remains a major clinical challenge. Here, we perform a comprehensive bioinformatic analysis of plasma proteomic profiles to explore the underlying biology of treatment resistance in NSCLC.

Methods The analysis was performed on 388 "resistance-associated proteins" (RAPs) that were previously described as pretreatment plasma proteomic predictors within the PROphet computational model designed to predict ICI clinical benefit in NSCLC. Putative tissue origins of the RAPs were explored using publicly available datasets. Enrichment analyses were performed to investigate RAP-related biological processes. Plasma proteomic data from 50 healthy subjects and 272 patients with NSCLC were compared, where patients were classified as displaying clinical benefit (CB; n=76) or no CB (NCB; n=196). Therapeutic agents targeting RAPs were identified in drug and clinical trial databases.

Results The RAP set was significantly enriched with proteins associated with lung cancer, liver tissue, cell proliferation, extracellular matrix, invasion, and metastasis. Comparison of RAP expression in healthy subjects and patients with NSCLC revealed five distinct RAP subsets that provide mechanistic insights. The RAP subset displaying a pattern of high expression in the healthy population relative to the NSCLC population included multiple proteins associated with antitumor activities, while the subset displaying a pattern of highest expression in the NCB population included proteins associated with various hallmarks of treatment resistance. Analysis of patient-specific RAP profiles revealed inter-patient diversity of potential resistance mechanisms, suggesting that RAPs may aid in developing personalized therapeutic strategies. Furthermore, examination of drug and clinical trial databases revealed that 17.5% of the RAPs are drug targets, highlighting the RAP set as a valuable resource for drug development.

Conclusions The study provides insight into the underlying biology of ICI resistance in NSCLC and

WHAT IS ALREADY KNOWN ON THIS TOPIC

⇒ Cancer resistance to immune checkpoint inhibitor (ICI) therapy is a major clinical challenge. The plasma proteome, reflecting tumor-related and immune-related activity, serves as a valuable source of information for elucidating the mechanisms underlying ICI resistance.

WHAT THIS STUDY ADDS

⇒ We performed a comprehensive bioinformatic analysis of pretreatment plasma proteomic profiles from 272 patients with metastatic non-small cell lung cancer, focusing on 388 "resistance-associated proteins" (RAPs) that form the basis of the PROphet model designed to predict clinical benefit in ICI-treated non-small cell lung cancer (NSCLC). The study provides insight into the biological processes associated with ICI resistance in NSCLC and highlights the potential clinical value of RAPs for developing personalized therapies.

HOW THIS STUDY MIGHT AFFECT RESEARCH, PRACTICE OR POLICY

⇒ Pretreatment plasma proteomic patterns reveal hallmarks of resistance to ICIs and represent a potential resource for developing personalized treatment strategies for NSCLC.

highlights the potential clinical value of RAP profiles for developing personalized therapies.

INTRODUCTION

Over the past decade, immune checkpoint inhibitors (ICIs) have emerged as pillars of cancer treatment, offering substantial therapeutic benefits and survival advantages over traditional cytotoxic chemotherapy alone. Unlike cytotoxic chemotherapy, ICIs augment an antitumor immune response by targeting checkpoint proteins such as programmed

cell-death protein-1 (PD-1), programmed death-ligand 1 (PD-L1), and cytotoxic T-lymphocyte associated protein-4 (CTLA-4) expressed on tumor and/or immune cells.[1] Clinical evidence shows that ICI efficacy varies widely between patients, with some achieving durable benefit and others displaying primary or acquired resistance.[2] Exploring tumor-host interplay in the context of ICI-based therapies is crucial for understanding the mechanisms behind this inter-patient variation and developing strategies to improve outcomes.

Currently, US Food and Drug Administration (FDA)-approved biomarkers for predicting outcomes and informing the use of ICIs include PD-L1 expression, tumor mutational burden (TMB), and microsatellite instability (MSI), all of which are related to the mechanism of action of ICIs.[3] However, it is widely acknowledged that biomarkers with more robust predictive capabilities are needed for optimal therapeutic decision-making. For example, for patients with oncogene driver-negative non-small cell lung cancer (NSCLC), a high PD-L1 tumor proportion score (TPS≥50%) provides eligibility for first-line PD-1/PD-L1 inhibitor monotherapy.[4] However, a study on real-world outcomes reported no clear association between PD-L1 expression and survival in patients with NSCLC receiving ICI monotherapy.[5] Although pembrolizumab has received tissue-agnostic approval for treating MSI-high or TMB-high solid tumors, studies have shown that the predictability of these biomarkers is not universal across or within tumor types.[6] Furthermore, while the KEYNOTE-158 trial showed that TMB-high cancers were associated with higher overall response rates, there was no association with an overall survival benefit.[7]

Plasma proteomics offers an attractive opportunity for the discovery of predictive biomarkers. Circulating blood contains thousands of proteins derived from the developing tumor, tumor microenvironment, peripheral immune cells, and other host cells. As such, the plasma proteome reflects tumor-intrinsic properties, immune cell dynamics, angiogenesis, extracellular matrix (ECM) remodeling, and metabolic changes,[8 9] making it a rich source of potential biomarkers. Such biomarkers can be sampled before or during treatment via a minimally invasive blood draw and measured using a single assay.

We recently reported the analytical and clinical validation of a plasma proteomics-based model termed PROphet.[10 11] The model computes the probability of achieving clinical benefit (CB, defined as progression-free survival at 12 months) from first-line PD-1/PD-L1 inhibitor-based therapies in patients with advanced NSCLC. The final model output, namely a PROphet-POSITIVE or PROphet-NEGATIVE result, successfully stratifies patients based on survival outcomes. Furthermore, for patients with PD-L1 TPS≥50%, the model distinguishes between those who benefit from ICI monotherapy and those for whom ICI-chemotherapy combinations are more effective. Conversely, the model identifies patients with PD-L1 TPS<1% likely to benefit

from ICI-chemotherapy combinations, offering much-needed guidance for clinical decisions regarding metastatic NSCLC management.

PROphet is based on 388 plasma proteins, collectively termed "resistance-associated proteins" (RAPs). During model development, RAPs were identified based on their differential pretreatment plasma levels in patients with NSCLC who achieved CB from ICI therapy versus those who did not. Thus, the RAP set represents a valuable source of information related to ICI therapeutic benefit and resistance in NSCLC.

Here, in this study, we performed a comprehensive bioinformatic exploration of the RAP set to understand the biological basis of our predictive model. This study provides insight into the biological processes associated with poor clinical outcomes. Our findings highlight the potential value of assessing the RAP profiles of individual patients for prognosis and treatment.

METHODS
Cohort description
NSCLC cohort: EDTA plasma samples were collected from patients with advanced-stage NSCLC with consent as part of the multicenter PROPHETIC study (NCT04056247). All sites received approval from the local institutional review board to perform the study before commencing (online supplemental table S1). Sample collection was previously described.[10 11] The patients received either ICI monotherapy (nivolumab, pembrolizumab, atezolizumab) or a combination therapy of ICI with chemotherapy. The clinical data were collected for each patient. CB was defined as progression-free survival at 12 months. Patients were classified as having either CB or no CB (NCB). The cohort for this study comprised 76 and 196 patients with CB and NCB, respectively. Demographics and clinicopathological characteristics were previously described, as the cohort corresponds to the patient subset used for blinded validation of the PROphet model (online supplemental table S2, adapted from a study by Christopoulos et al,[11] with permission from the publisher).

Healthy cohort: Samples from healthy subjects were collected at two centers: Roswell Park Cancer Center Biobank and Baylor Scott and White Research Institute. Fifty samples from healthy subjects were examined.

Integration of NSCLC and healthy cohorts: To verify that the NSCLC and healthy cohorts were balanced and suitable for integrated analysis, basic clinical parameters, namely sex and age, were compared between the two cohorts. Kolmogorov-Smirnov test and Student's t-test were applied to examine potential differences in age distribution and average, respectively (Kolmogorov-Smirnov test p value=0.08; two-sided t-test p value=0.17). A χ^2 test was used to compare sex categories between the two cohorts (p value=0.09). Lastly, a two-way analysis of variance was applied to examine the potential association between the two clinical parameters (p value=0.13). Based on these analyses, the two cohorts did not display

significant differences in these clinical parameters and could thus be integrated for analysis (n=322; online supplemental figure S1).

Proteomics measurement

Proteomic profiling of all plasma samples was performed using the SomaScan Assay V.4.1, SomaLogic (Boulder, Colorado, USA). The assay is based on Slow Off-Rate Modified Aptamers (SOMAmers).[12] The SomaScan proteomic dataset, comprizing 7596 aptamers, was narrowed to 1578 proteins with high analytical reliability, as described in detail.[11] The measurements were taken from distinct samples.

Data analysis

All analyses were performed on log2 transformed measurement values of the proteomic data. Data analyses were conducted using Python, Perseus Computational Platform,[13] and GraphPad (San Diego, California, USA, http://www.graphpad.com). Plots were generated using matplotlib and seaborn packages. Hierarchical clustering was performed using the scikit-learn Python package. The Ward algorithm was used for hierarchical clustering. For functional interaction analysis, the Search Tool for the Retrieval of Interacting Genes/Proteins (STRING) tool was used under default conditions.[14] Voronoi plots for the RAPs were plotted using Proteomaps.[15] Biomarkers were identified using the CIViCmine database focusing on lung cancer biomarkers based on the following categories: "protein expression", "overexpression", "under expression", and "expression".[16]

Enrichment analyses were performed using Fisher's exact test (Benjamini-Hochberg false detection rate (FDR)<0.1) based on the 1578 proteins as the background. The databases used for enrichment analysis for a potential source of the RAPs are indicated in online supplemental table S3. Specifically, protein expression in normal tissues is based on Human Protein Atlas (HPA) data (http://www.proteinatlas.org) using protein evidence categories (HPA; HPA & UniProt & Proteogenomics; HPA & UniProt; HPA & Proteogenomics; Proteogenomics), where expression in specific tissues was based on "Tissue enhanced" or "Tissue enriched" categories. "Expressed in all tissues" was used for expression in all normal tissues. For expression in immune cells, the HPA database was used based on RNA expression data from different immune cells. Lung cancer-related proteins were defined using the HPA and Clinical Proteomic Tumor Analysis Consortium (CPTAC) data as follows. HPA data were obtained from pathology data, where proteins were defined as lung cancer-related when≥50% of the tumor samples had high expression levels. From the CPTAC data, a protein was defined as adenocarcinoma or squamous cell carcinoma lung cancer-related. Functional groups were derived from the Gene Ontology (GO) resource, the Kyoto Encyclopedia of Genes and Genomes (KEGG) resource, keywords, and the Cancer Hallmarks Analytics Tool resource. ECM-related proteins

were obtained using GO categories or the Matrisome project. Proteins related to blood proteome-based lung cancer diagnosis were identified based on a study by The Lung Cancer Cohort Consortium. Correlations between protein expression data and body mass index (BMI), lactate dehydrogenase (LDH), and C-reactive protein (CRP) were performed for patients with NSCLC with available data; 137, 102, and 90 patients had data for BMI, LDH, and CRP, respectively.

Student's t-test was performed to compare proteomic data from patients classified with poor or good prognosis, based on the following factors: PD-L1 level (low or negative vs high), age (>75 vs ≤75), the Eastern Cooperative Oncology Group (ECOG) performance status (1–2 vs 0), histology (squamous vs non-squamous), liver metastasis (yes vs no), brain metastasis (yes vs no), bone metastasis (yes vs no), smoking status (never smoker vs current smoker; ex-smokers were excluded), neutrophil-to-lymphocyte ratio (NLR; NLR≥4 vs <4), TMB (low vs high), STK11 mutation (yes vs no) and KEAP1 mutation (yes vs no). All t-tests were performed under the same conditions (permutation-based FDR<0.1). Enrichment of RAPs among the liver metastasis differentially expressed proteins was examined using Fisher's exact test (FDR<0.1).

Clustering and pattern analysis

The expression levels were normalized using Z-score, and the median expression level of core RAPs per subcohort (NSCLC CB, NSCLC NCB, and healthy subjects) was calculated. Unsupervised hierarchical clustering analysis was performed to obtain 15 clusters. The clusters were combined to obtain five different patterns for further analyses. The association between the expression level of each RAP and BMI, LDH blood level, and CRP blood level in patients with NSCLC was calculated using Spearman's correlation.

Clinical targeting of RAPs

Direct interactions between RAPs and drugs were investigated using the Drug-Gene Interaction database (DGIdb),[17] updated in February 2022. The interactions identified primarily from the National Cancer Institute (NCI) database were further confirmed using other databases, such as the Open Target and Gene Card Drug Modules. These validated interactions were then categorized into one of five categories using the FDA.gov and ClinicalTrial.gov websites. The five categories are: FDA approved for non-cancer indications, FDA approved for cancer, FDA approved for NSCLC, investigational new drug (IND) for other cancer types, and IND for NSCLC. Patient-specific resistance profiles were generated as follows: RAPs from patterns D and E were characterized according to their involvement in four resistance-related processes: angiogenesis, cell proliferation, chemoresistance, and immune-related processes. RAP expression was normalized using Z-score. For each patient, the median normalized

expression level of the RAPs assigned to a resistance-related process represented the score.

RESULTS

Biological functions and potential cellular origins of RAPs

The PROphet model relies on 388 RAPs selected based on their differential distributions in pretreatment plasma samples of patients with NSCLC who achieved CB versus NCB from PD-1/PD-L1 inhibitor-based therapies, either alone or in combination with chemotherapy. During model development, RAPs were selected using a cross-validation process that defines the weight of each RAP based on its selection frequency.[11] In the current study, "core RAPs" were defined as those selected ≥10 times during cross validation. Of the 388 RAPs, 113 were categorized as "core" (online supplemental figure S2 and online supplemental table S4).

To gain a broad view of the potential biological processes driven by RAPs, we explored the entire RAP set using Proteomaps[15] and functional enrichment analysis. Multiple RAPs were found to be involved in metabolic processes (including glycolysis, glycan metabolism, and cofactor biosynthesis), complement and coagulation cascades, splicing, cell cycle, and various signaling cascades (figure 1A). Pathway enrichment analysis revealed several cancer-related processes, including proliferative signaling, ECM-related processes, tumor-promoting inflammation, invasion, and metastasis (Fisher's exact test, FDR<0.1; figure 1B and online supplemental table S5A). Core RAPs displayed similar enrichment results (Fisher's exact test, FDR<0.1; online supplemental figure S3 and online supplemental table S5B).

To identify the potential tissues or cell types from which RAPs originate, we characterized RAPs using publicly available databases (HPA and CPTAC). Of all RAPs, 10%, 36%, and 43% were potentially associated with lung cancer, immune cells, and normal tissue expression profiles, respectively, suggesting that RAPs originate from both tumor and host tissues (figure 1C). Similar proportions were observed within a set comprizing only core RAPs (online supplemental figure S4A). Notably, the RAP set was significantly enriched with proteins related to lung cancer and normal liver tissue (Fisher's exact test, FDR<0.1; figure 1D and online supplemental table S6A), whereas core RAPs displayed similar results without liver
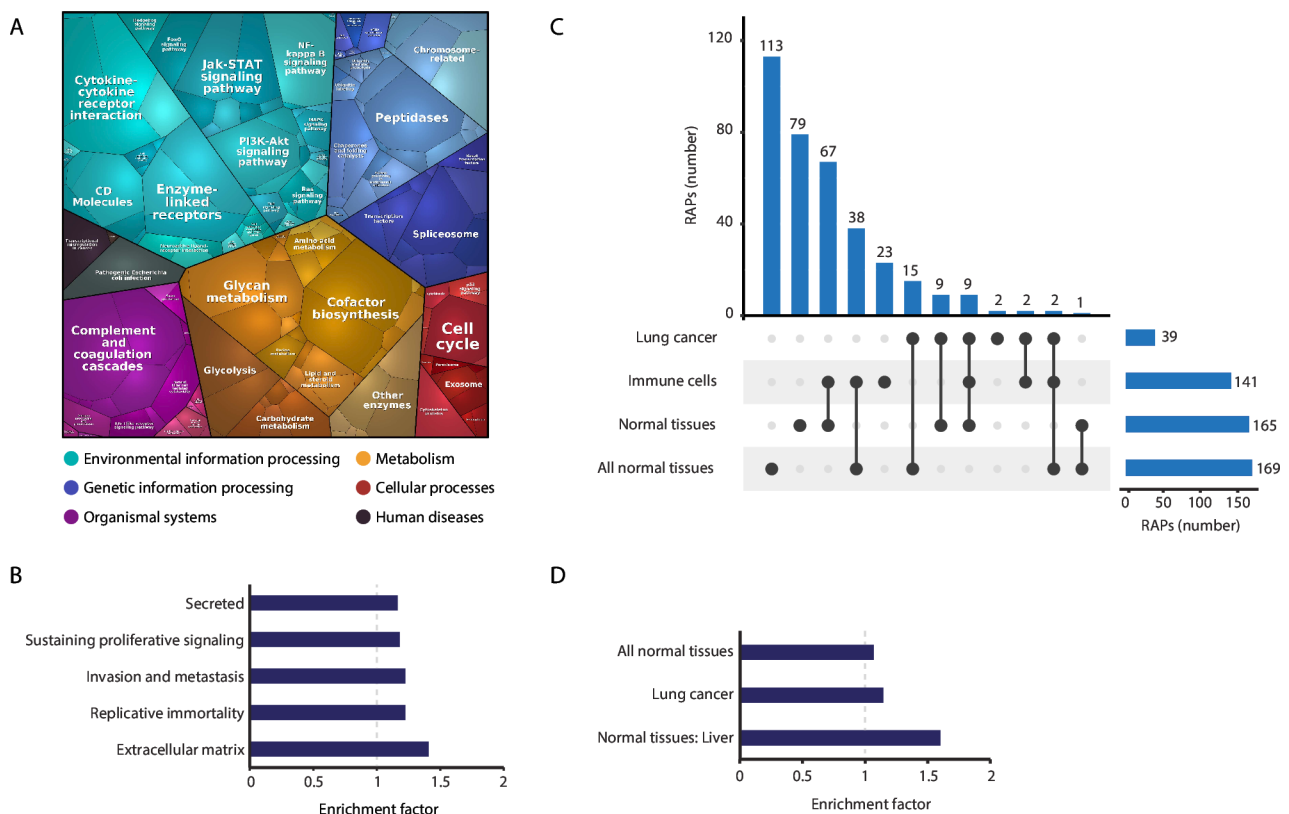

Figure 1 Biological functions and potential cellular origins of resistance-associated proteins (RAPs). (A) Voronoi plot displaying the main biological processes in which RAPs may be involved. Each polygon represents a RAP. Polygon size is correlated with RAP weight. RAPs were categorized into six main categories based on the KEGG (Kyoto Encyclopedia of Genes and Genomes) database. The plot was generated using the Proteomaps tool. (B) Enrichment analysis of functional categories (Fisher's exact test, false detection rate (FDR)<0.1). (C) RAPs were categorized based on expression data from the CPTAC (Clinical Proteomic Tumor Analysis Consortium) and HPA (Human Protein Atlas) databases, as described in Methods. The diagram shows the number of RAPs in each category (horizontal bars) and the number of RAPs unique to each category or common to more than one category (vertical bars). (D) Enrichment analysis of potential sources of RAPs (Fisher's exact test; FDR<0.1).

enrichment (online supplemental figure S5B and online supplemental table S6B).

Several lung-cancer-related RAPs were functionally connected (figure 2A), suggesting they may be involved in similar biological processes. Indeed, this RAP subset displayed significant enrichment of proteins associated with various hallmarks of cancer (ie, evading growth suppressors, resisting cell death, invasion, and metastasis), ECM, and poor prognosis in lung cancer (Fisher's exact test, FDR<0.1; figure 2A and online supplemental table S7). Among the lung cancer-related RAPs, SERPINB5 (serpin B5), GREM1 (gremlin 1), POSTN (periostin), and KRT18 (keratin 18) were previously reported to be associated with poor prognosis in lung cancer (HPA database). Furthermore, most lung cancer-related RAPs displayed higher expression levels in the plasma of patients with NSCLC than in that of healthy subjects (figure 2B). Some lung cancer-related RAPs were found to be specifically associated with lung squamous cell carcinoma and/or lung adenocarcinoma based on the CPTAC datasets (figure 2B). There are several proteins of interest among the lung cancer-related RAPs. For example, SFN (stratifin) is an adapter protein involved in cell cycle, cell adhesion, and migration and has an established role in lung cancer development and progression.[18] Overall, these findings highlight the biological significance of this RAP subset and support a lung cancer origin for several RAPs.

Liver-related RAPs were highly interconnected in a functional interaction network (online supplemental figure S5A). In terms of cellular origin, enrichment analysis revealed a potential hepatocyte origin as opposed to the other examined liver cell types (enrichment factor=5.1287, FDR=4.92E-15, Fisher's exact test; online supplemental figure S5A and online supplemental table S8A). The liver-related subset was significantly enriched with proteins related to the acute phase response, fibrinolysis, coagulation, complement system, lipid metabolism, and tumor-related characteristics, including ECM and cell proliferation (Fisher's exact test, FDR<0.1; online supplemental figure S5A and online supplemental table S8B). To investigate whether the enrichment of liver-related proteins among RAPs is driven by liver metastasis, we compared the plasma proteomic profiles of patients with and without liver metastasis (patient numbers are shown in online supplemental table S2). There was only one liver-related RAP among the proteins displaying differential expression in the two patient groups, suggesting that liver metastasis is not the likely cause of this enrichment (online supplemental figure S5B and online supplemental table S9). Notably, there was a significant enrichment of RAPs among the proteins displaying differential expression in patients with and without liver metastasis (19 RAPs out of 31 differentially expressed proteins, p value=4.39E-06). Several of these RAPs are known to be associated with immunosuppression (eg, SPINT1 (serine peptidase inhibitur Kunitz type 1) and EPHA10 (EPH receptor A10) are related to M2 macrophages; EPHB4 (EPH receptor B4) and HAVCR1, (Hepatitis A virus cellular receptor 1) are related to regulatory T-cells).

Overall, these findings highlight lung cancer, the liver, and immune cells as potential sources of circulating RAPs. They also suggest an association between RAPs and biological processes related to cancer progression, immunosuppression, and treatment resistance.

Association between RAPs and prognostic factors

To investigate whether RAPs are associated with known prognostic factors, proteomic data were analyzed after classifying patients into poor prognosis versus good prognosis groups based on the following 12 clinical or pathological factors: tumor PD-L1 level (low or negative vs high), age (>75 vs ≤75), ECOG performance status (1–2 vs 0), histology (squamous vs non-squamous), liver metastasis (yes vs no), brain metastasis (yes vs no), bone metastasis (yes vs no), smoking status (never smoker vs current smoker), NLR (≥4 vs <4), TMB (low vs high), STK11 (Serine/Threonine Kinase 11) mutation (yes vs no) and KEAP1 (Kelch-like ECH-associated protein 1) mutation (yes vs no). The latter two mutations were recently reported to be associated with immunosuppression.[19] RAPs displaying significant differences in expression between poor prognosis and good prognosis patient groups were identified using a t-test per prognostic factor category. Overall, 72 RAPs (of which 37 were core RAPs) passed at least one t-test (FDR<0.1, figure 3). Of the 37 core RAPs, most displayed significance for only one prognostic factor category, suggesting that different RAP subsets reflect distinct mechanisms related to prognosis. In 5 of the 12 categories, namely age, ECOG, histology, liver metastasis, and brain metastasis, all the significant RAPs displayed higher expression levels in the poor prognosis group, mostly coinciding with the expression pattern derived from the NCB versus CB comparison. In contrast, the PD-L1 category displayed an opposite trend. For the remaining six prognostic factor categories, namely bone metastasis, smoking, NLR, TMB, STK11, and KEAP1, none of the RAPs showed significant differences. However, such results should be interpreted with caution as patient numbers were low in some cases (eg, five never smokers and only a few patients with KEAP1 or STK11 mutations). Overall, these findings highlight associations between RAPs and different prognostic factors. Further analysis in a larger cohort may reveal mechanistic insights into patient prognosis.

Biological insights from RAP expression patterns in healthy subjects and patients with NSCLC

To gain further biological insights, we explored the relative expression of RAPs in healthy subjects and patients with NSCLC displaying CB or NCB. For this analysis, we focused on core RAPs (n=113), representing predictors with greater weight, given their higher stability during the RAP selection process.[11] Hierarchical clustering based on the median normalized RAP expression in healthy, CB, and NCB populations revealed 15 clusters (figure 4A,
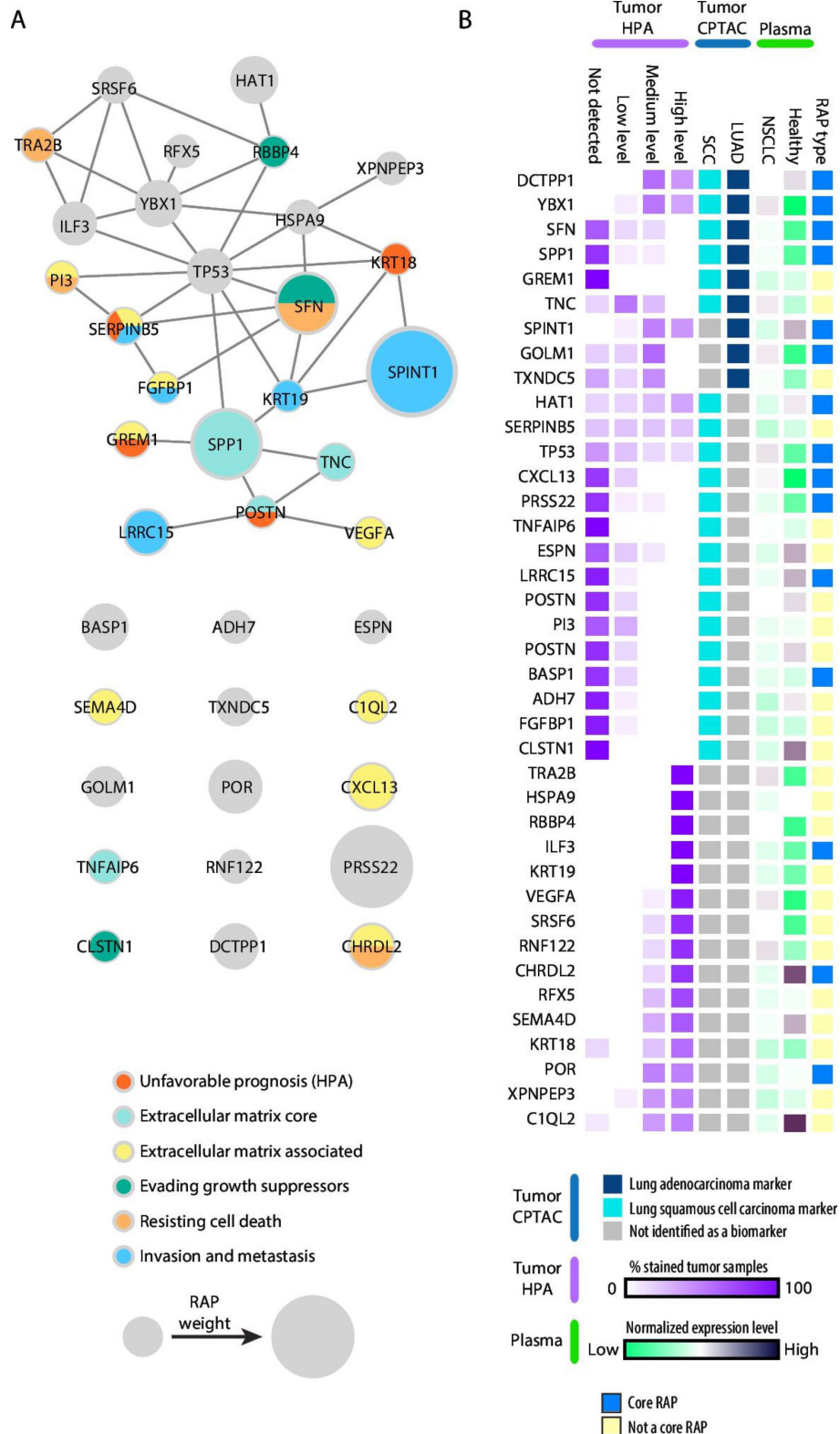
Figure 2 Functional analysis of lung cancer-related resistance-associated proteins (RAPs). (A) Functional network of lung-cancer-related RAPs. The network is based on the Search Tool for the Retrieval of Interacting Genes/Proteins (STRING) database. The node colors indicate different enriched biological categories. RAP weight is indicated by node size. (B) Heatmap displaying the lung cancer-associated RAPs based on (1) the Human Protein Atlas (HPA) database and (2) the National Cancer Institute's Clinical Proteomic Tumor Analysis Consortium (CPTAC) lung tumor publications. The fraction of lung cancer samples with expression levels in each HPA category is indicated in purple (categories are "not detected", "low", "medium", and "high" levels). Lung squamous cell carcinoma (SCC) and lung adenocarcinoma (LUAD) datasets were used in the CPTAC database. Each RAP's median normalized expression level is indicated for the non-small cell lung cancer (NSCLC) and healthy subject datasets.
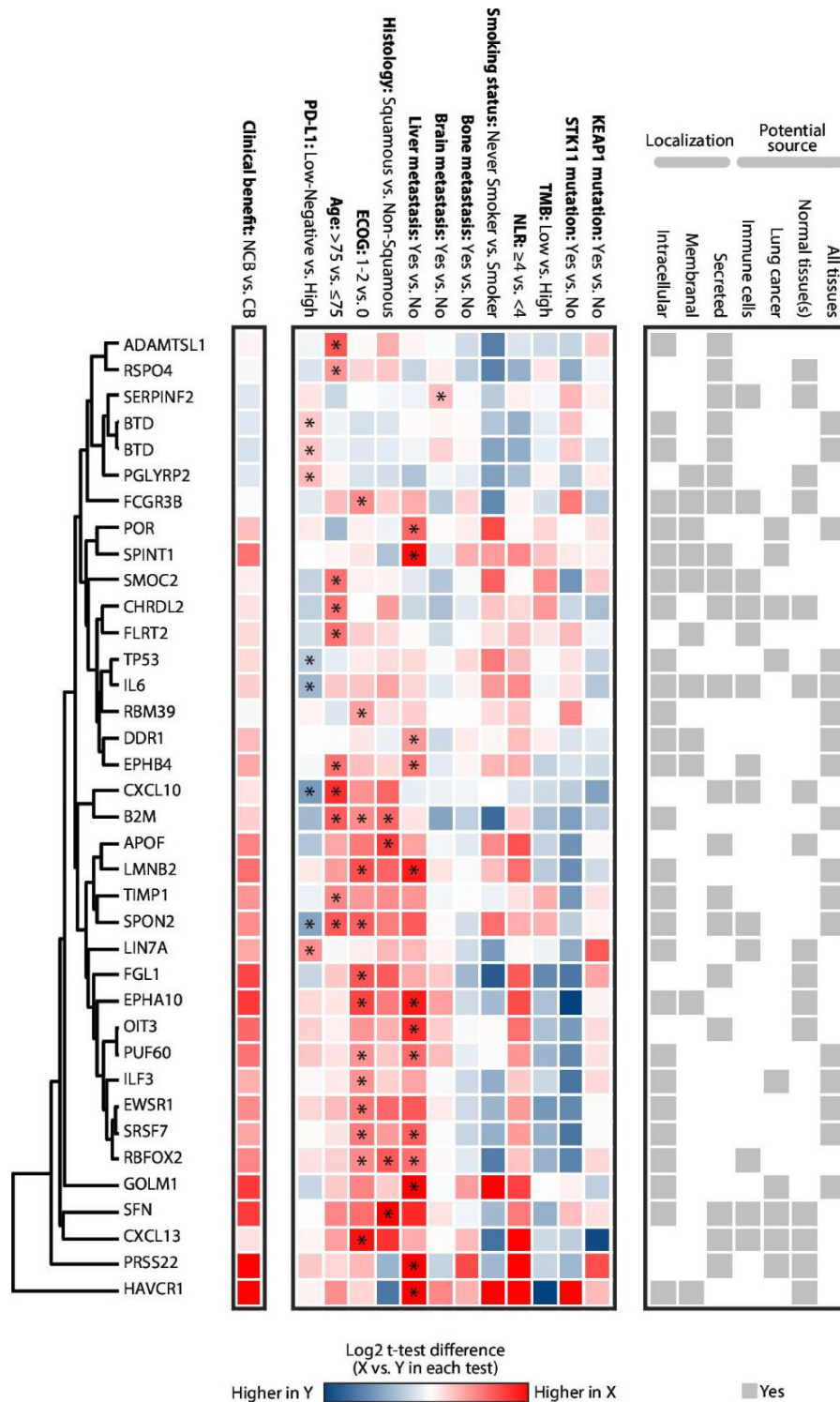
Figure 3 Association between core resistance-associated proteins (RAPs) and prognostic factors. A Student's t-test was performed to compare protein expression data from patients classified into poor prognosis and good prognosis groups based on 12 known prognostic factors, as indicated in the figure. The heatmap displays the t-test difference between the poor prognosis group (designated X) versus the good prognosis group (designated Y). The red-blue color scale denotes protein expression level, where red and blue indicate higher expression in X and Y, respectively. Core RAPs that passed at least one t-test are displayed. Significance is indicated by an asterisk. For reference, the t-test difference between the no clinical benefit (NCB) versus clinical benefit (CB) subpopulations is displayed on the left. A red-blue color scale is used, where red and blue indicate higher expression in NCB and CB populations, respectively. Protein localization and potential source are indicated in the panel on the right. ECOG, Eastern Oncology Cooperative Group; KEAP1, Kelch like ECH-associated protein 1; NLR, neutrophil-to-lymphocyte ratio; PD-L1, Programmed death-ligand 1; STK11, Serine/Threonine Kinase 11; TMB, tumor mutational burden.
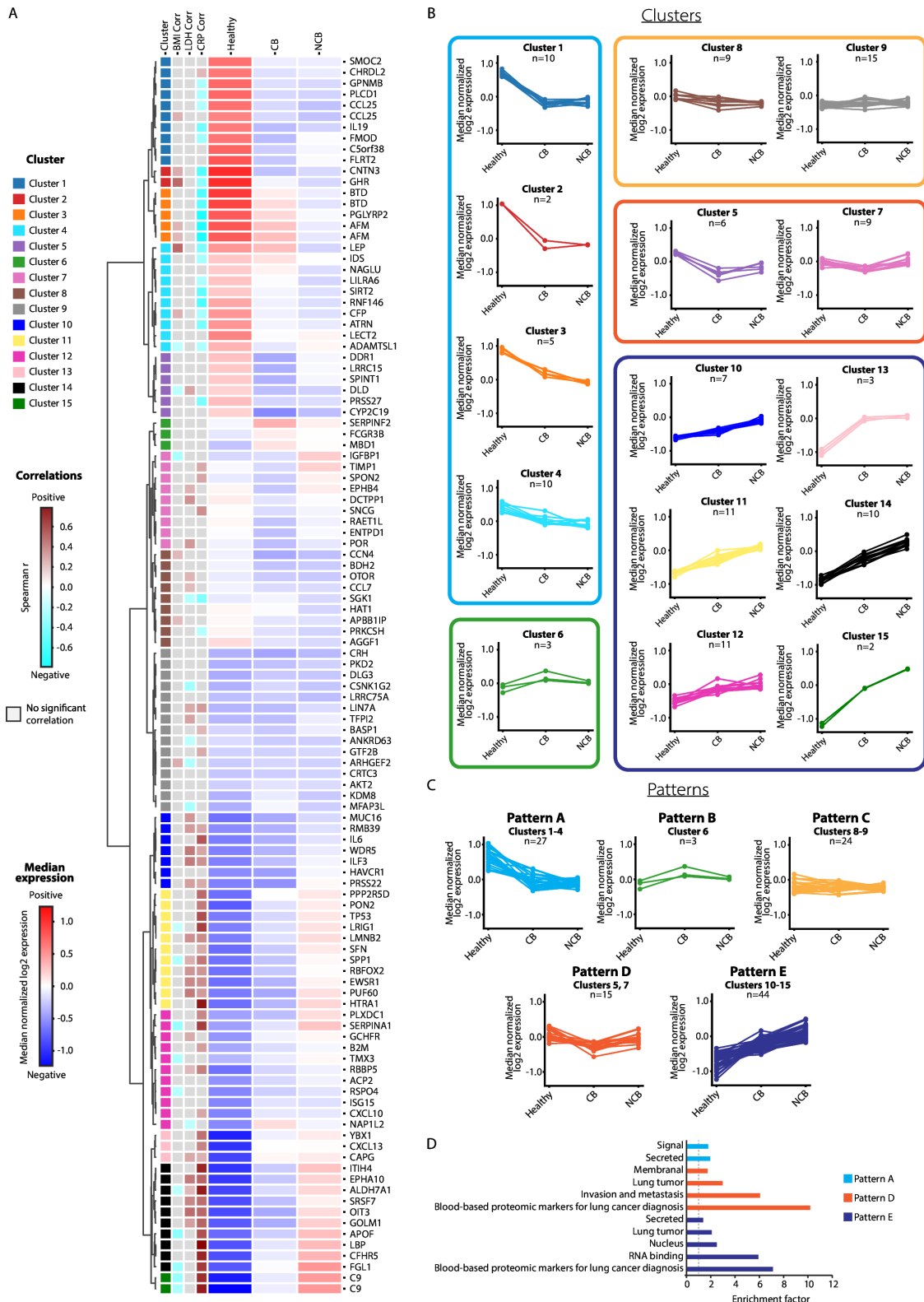
Figure 4 Hierarchical clustering analysis of resistance-associated protein (RAP) expression in patients with non-small cell lung cancer (NSCLC) and healthy subjects. (A) Unsupervised hierarchical clustering of core RAPs (n=113) was based on median Z-scored normalized RAP plasma levels in healthy subjects (n=50) and patients with NSCLC displaying clinical benefit (CB; n=76) or no clinical benefit (NCB; n=196). Each RAP was assigned to one of the 15 clusters, as indicated by the color. For each RAP, the light blue to brown scale indicates the correlations between RAP expression levels and body mass index (BMI), lactate dehydrogenase (LDH), or C-reactive protein (CRP). (B) The 15 clusters were further grouped according to relative RAP expression in healthy, CB, and NCB populations. (C) Five expression patterns were identified based on 15 clusters. (D) Enrichment analysis for each of the five patterns (Fisher's exact test, false detection rate<0.1). These categories are described in detail in Methods in data analysis section.

online supplemental table S10). Next, in the NSCLC cohort, we assessed the correlations between the plasma levels of each RAP and clinical parameters previously shown to be associated with ICI outcomes, namely BMI, LDH, and CRP. RAPs displaying a positive correlation with BMI were highly expressed in healthy subjects (ie, those clustered at the top of the heatmap). Conversely, RAPs displaying a negative correlation with BMI mainly corresponded to highly expressed RAPs in patients with NCB (ie, those clustered at the bottom of the heatmap). An opposite trend to that of BMI was observed for CRP, with negative correlations among RAPs highly expressed in healthy subjects and positive correlations among RAPs highly expressed in patients with NCB. For LDH, positive correlations were mostly found among RAPs highly expressed in patients with NCB (figure 4A). These findings are consistent with previous studies reporting an association between high BMI and ICI therapeutic benefit,[20] and associations between high blood levels of LDH or CRP with poor outcomes from ICI therapies.[21]

The 15 clusters were further grouped according to relative RAP expression in healthy, CB, and NCB populations. Five distinct expression patterns were detected: Patterns A, B, C, D, and E (figure 4B,C). Pattern A was characterized by higher RAP expression in the healthy population than in the NSCLC population. Pattern B included RAPs with higher expression in the CB population. Patterns D and E displayed higher RAP expression in the NCB population than in the CB population, differing from each other in relation to the healthy population. Pattern C displayed no clear trends. Given the above-described trends, we further explored the RAP composition of patterns A, B, D, and E regarding their potential roles in health, cancer, and clinical outcomes.

High expression in healthy subjects (pattern A)
Pattern A comprised 23 RAPs displaying elevated expression in healthy subjects relative to CB and NCB patients with NSCLC, suggesting that these proteins differentiate between healthy and cancerous states. These include AFM (Afamin), CNTN3 (Contactin 3), and LECT2 (Leukocyte Cell Derived Chemotaxin 2), all of which were previously shown to be downregulated in sera or plasma from patients with NSCLC compared with healthy controls,[22] which is in agreement with the expression patterns shown here. Cluster 3, assigned to pattern A, displayed a trend of highest expression in healthy subjects and lowest in NCB patients. It comprises AFM (identified by two aptamers), PGLYRP2 (Peptidoglycan recognition protein 2; a liver-associated proteins), and BTD (biotinidase). AFM, a member of the albumin protein family, serves as an alternative vitamin E transporter. Since vitamin E has been shown to enhance ICI efficacy,[23] elevated AFM levels may be associated with treatment outcomes. PGLYRP2 is a bacterial peptidoglycan-sensing pattern recognition receptor that stimulates an antitumor immune response in hepatocellular carcinoma.[24] The antitumor roles of such proteins align with their upregulation in healthy

subjects and their downregulation in patients with NCB. Another RAP of particular interest in this pattern is LEP (leptin), a pro-inflammatory adipokine strongly correlated with BMI[25] and has been shown to enhance antitumor immunity.[26] In our NSCLC cohort, LEP levels were highly correlated with BMI (online supplemental figure S6A). Its significantly decreased level in NCB patients compared with that in CB patients aligns with its reported antitumor role (online supplemental figure S6B). Enrichment analysis of pattern A RAPs showed that this set was significantly enriched with signaling and secreted proteins (Fisher's exact test, FDR<0.1; figure 4D and online supplemental table S11A).

High expression in CB patients (pattern B)
Pattern B consisted of three RAPs (SERPINF2, MBD1, and FCGR3B) with higher expression in the CB population than in the NCB population and healthy subjects. SERPINF2 (A2AP) is an essential regulator of fibrinolysis and the complement system and was recently shown to be elevated in the plasma of hepatocellular carcinoma patients who respond to PD-1 inhibitor plus lenvatinib combination therapy.[27] MBD1 (Methyl-CpG Binding Domain Protein 1) has dual roles as a tumor suppressor and oncogene, depending on the cancer type.[28] FCGR3B (CD16B) is often considered an activating Fc receptor that can induce antibody-dependent cellular cytotoxicity and antibody-dependent cellular phagocytosis, which may assist in the immune response.[29]

High expression in healthy subjects and NCB patients (pattern D)
Pattern D is characterized by high RAP expression in healthy and NCB populations relative to the CB population. Among these RAPs are known tumor-supporting factors, including CD39 (encoded by ENTPD1), an ectonucleotidase that converts extracellular ATP to immunosuppressive adenosine, thereby leading to dampened antitumor immunity[30]; EPHB4, a receptor tyrosine kinase implicated in cancer progression, metastasis, and angiogenesis[31]; SPON2, an ECM protein with diagnostic and prognostic value for several cancers[32]; and TIMP1, a matrix metalloproteinase inhibitor that plays a critical role in regulating cell proliferation, angiogenesis, apoptosis, and differentiation, as well as shaping an immunosuppressive microenvironment.[33] Elevated levels of such proteins in healthy subjects may reflect physiological roles unrelated to cancer (eg, immune suppression under normal conditions by CD39). In contrast, increased expression in NCB patients is likely related to their immunosuppressive and pro-tumorigenic roles. Notably, pattern D proteins exhibited significant enrichment in pathways related to invasion and metastasis, in line with the upregulation of these proteins in patients with NCB compared with those with CB, as well as blood-based proteomic markers implicated in lung cancer diagnosis (Fisher's exact test; FDR<0.1; figure 4D, online supplemental figure S7 and online
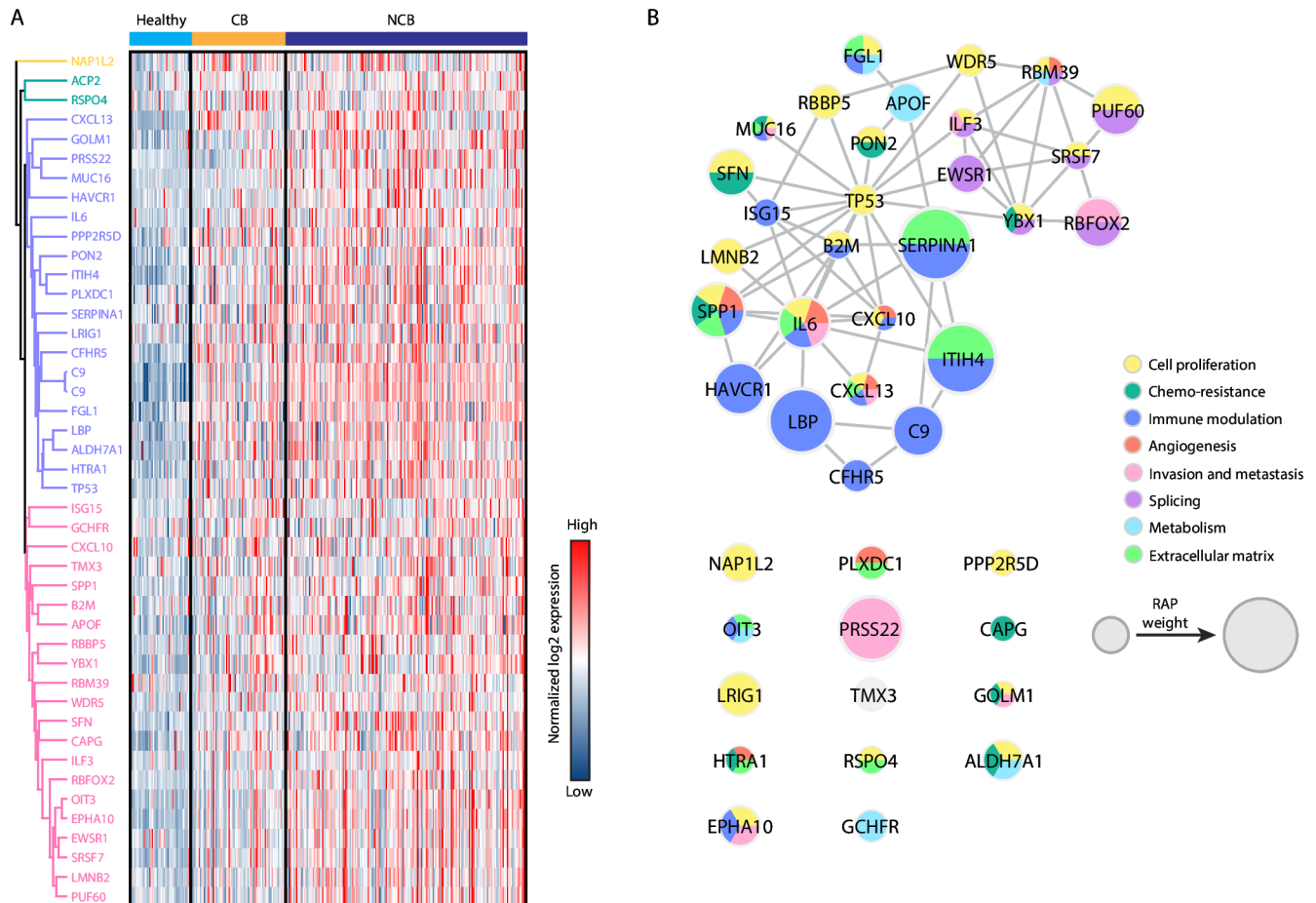
Figure 5 Resistance-associated proteins (RAPs) upregulated in patients with no clinical benefit (NCB) are associated with distinct biological processes. (A) Heatmap displaying the plasma levels of pattern E RAPs in healthy subjects and patients with non-small cell lung cancer with clinical benefit (CB) or NCB. Each row corresponds to a RAP. Each column represents a subject or patient. The red-blue color scale indicates RAP expression. (B) Functional network of Pattern E RAPs. The network is based on the Search Tool for the Retrieval of Interacting Genes/Proteins (STRING) database. Different biological categories are indicated by node color. RAP weight is indicated by node size.

supplemental table S11A,B). The latter category, which displayed the most pronounced enrichment, is based on 36 highly expressed proteins in lung cancer patients from a large case–control study; two of the 15 pattern D proteins (SPINT1 and IGFBP1) are found among the 36 lung cancer diagnostic markers.

High expression in NCB patients (pattern E)

Pattern E, representing the largest group, comprised 44 RAPs that displayed relatively low expression in the healthy population, intermediate expression in the CB population, and high expression in the NCB population (figure 5A), suggesting that this subset contains potential lung cancer biomarkers associated with tumor progression and treatment resistance. Indeed, pattern E proteins were significantly enriched in multiple categories, including lung cancer-related proteins, proteins associated with RNA binding, and blood-based proteomic markers implicated in lung cancer diagnosis (Fisher's exact test, FDR<0.1; figure 4D, online supplemental figure S7 and online supplemental table S11A,B). Four

blood-based proteomic markers were identified among pattern E RAPs (MUC16, IL6, CXCL13, and CFHR5).

In the protein interaction network, pattern E RAPs were arranged into three main groups (figure 5B). The first group consists of splicing-related proteins, which may be relevant considering the potential role of abnormal splicing in promoting resistance to different types of cancer therapies, including ICIs.[34] The second group, with TP53 as its hub, involves proteins related to cell proliferation. One of them is MUC16 (CA125), a widely used screening tumor biomarker that is elevated in the sera of patients with advanced NSCLC and is associated with poor prognosis.[35] The third group was predominantly comprised of immunomodulatory proteins, including (1) acute phase response proteins such as IL6 (at the hub), SERPINA1, ITIH4, and LBP, consistent with the connection between acute phase response and ICI resistance[36]; (2) complement proteins such as C9 and CFHR5, in line with complement-mediated immunosuppressive activities that support tumor progression[37]; and (3) immunomodulatory proteins associated with ICI resistance, possibly

owing to their role in immune evasion. For example, oste-opontin (OPN, encoded by SPP1) is a known tumorigenic and metastatic factor that acts as a potent suppressor of antitumor immunity by binding CD44 on T cells.[38] TIM-1 (encoded by HAVCR1) is upregulated in multiple cancer types and shows a positive correlation with poor prog-nosis.[39] FGL1 is a liver-secreted protein that inhibits T-cell activation by acting as a ligand of the immune checkpoint protein LAG3. Elevated FGL1 levels in plasma are associ-ated with poor prognosis and resistance to PD-1/PD-L1 inhibitors in patients with NSCLC.[40] CXCL10 is a cyto-kine involved in multiple processes, including the differ-entiation and activation of peripheral immune cells, cell chemotaxis, regulation of cell growth, angiogenesis, and apoptosis. Furthermore, multiple studies have identified it as a protein involved in the response to ICI-based treat-ment, either positively or negatively.[9 41] Finally, high circu-lating levels of beta-2 microglobulin (encoded by B2M), a component of the major histocompatibility complex (MHC) class I antigen presentation machinery, correlate with resistance to ICI-based therapies in both NSCLC and melanoma.[42] Overall, pattern E RAPs cover a range of immune-related and non-immune-related mechanisms that potentially drive tumor progression and resistance to ICIs.

In summary, grouping RAPs according to their rela-tive expression in healthy subjects, patients with CB, and patients with NCB provides insight into potential resis-tance mechanisms. Specifically, patterns D and E RAPs, characterized by higher expression in NCB patients than in CB patients, were associated with various biological processes contributing to treatment resistance via diverse mechanisms (figure 6).

Patient-level RAP profiles provide insights into personalized treatments

Combining standard ICI-based treatments with thera-peutic agents that target specific resistance mechanisms is a potential strategy to improve outcomes in patients who are unlikely to benefit from standard therapies. Therefore, identifying the resistance mechanisms and the proteins that drive them may guide the rational design of such combination therapies.[43] To explore the clinical potential of this strategy in the context of RAPs, we exam-ined drug and clinical trial databases for therapeutic drugs that target individual RAPs. The drugs were catego-rized according to their status (ie, FDA-approved drug vs IND) and the disease indicated (ie, NSCLC, other cancer types, and non-cancer indications). The analysis showed that 17.5% and 18.3% of all RAPs and core RAPs, respec-tively, were targeted by drugs in at least one category (figure 7A,B and online supplemental table S12). Eight RAPs were targets of FDA-approved drugs for NSCLC or other cancers, while 36 RAPs were associated with FDA-approved drugs for non-cancer indications. Of the 32 RAPs targeted by INDs for different cancer types, 17 are relevant for NSCLC, in addition to 4 RAPs being targets of INDs solely for NSCLC. These findings demonstrate the availability of an extensive repertoire of RAP-targeting drugs that could potentially be incorporated into novel, rational combination treatments to address resistance to ICI-based therapies.

We further speculated that the RAP profiles of indi-vidual patients may shed light on patient-specific resis-tance mechanisms. To explore this possibility, we first characterized RAPs based on their involvement in four
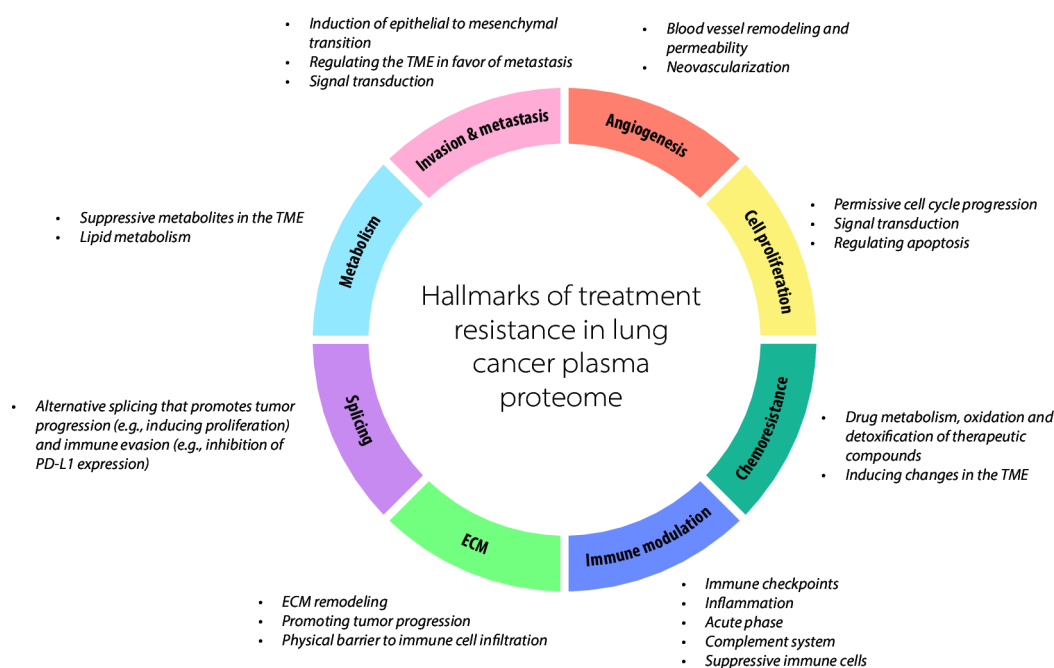

Figure 6 Hallmarks of the no clinical benefit plasma proteome. Resistance-associated proteins from the pattern D and E subsets are involved in eight main processes that may contribute to tumor progression and treatment resistance in different ways. ECM, extracellular matrix; PD-L1, programmed death-ligand 1; TME, tumor microenvironment.
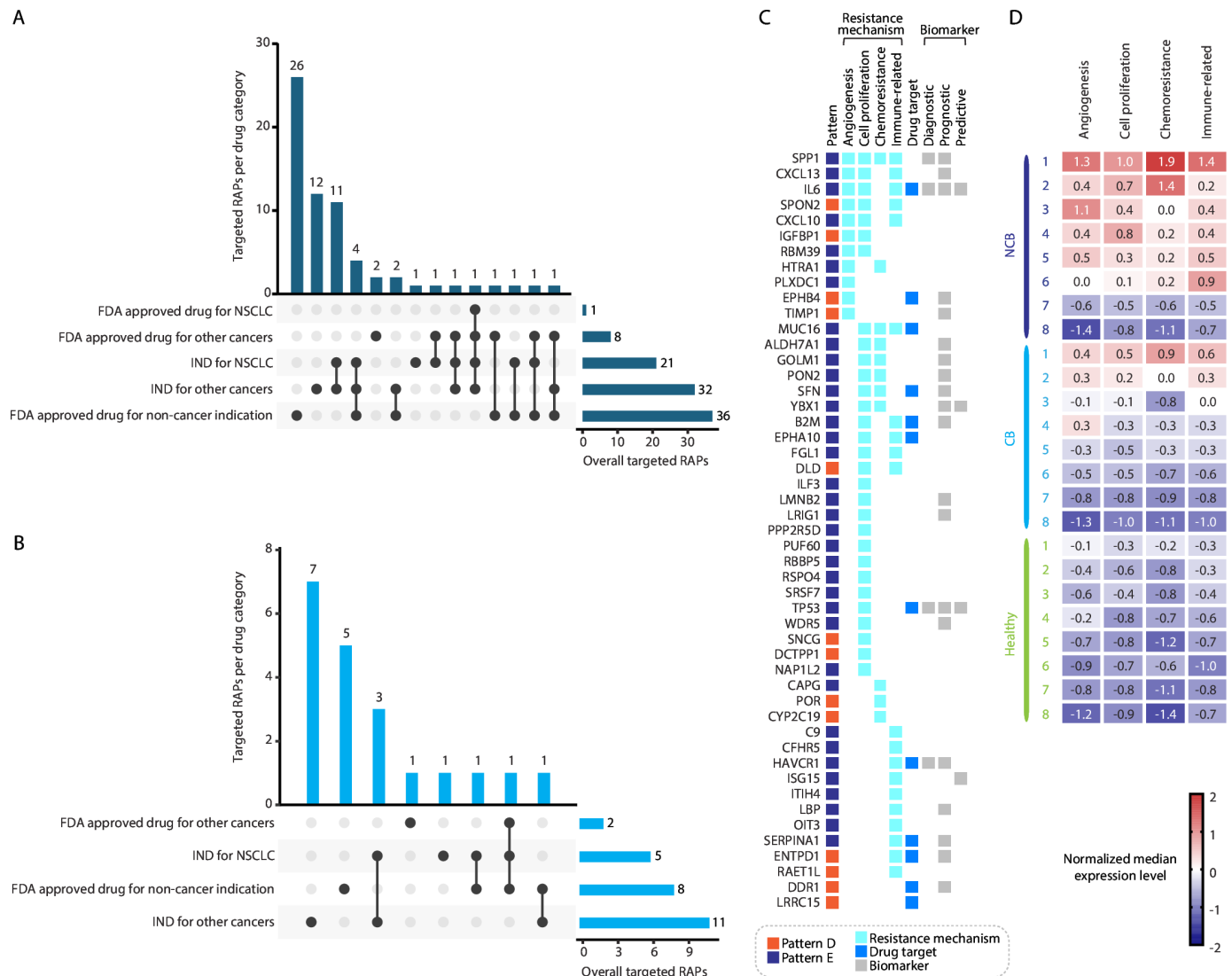
Figure 7 Clinical relevance of patient-level resistance-associated protein (RAP) profiles. (A–B) Drug and clinical trial databases were screened for therapeutic drugs that target individual RAPs. Drugs were categorized according to their status and indications. The number of drugs targeting RAPs is summarized per drug category for the entire RAP set (A) and core RAPs (B). (C) Pattern D and E RAPs were categorized according to their involvement in the four resistance mechanisms, as indicated. RAPs that represent drug targets or cancer biomarkers are also indicated. Of the patterns D and E RAPs, only those assigned to one or more of the indicated categories are displayed. (D) Resistance profiles for individual patients were generated by scoring each resistance mechanism. The scores were based on the median normalized expression levels among the RAPs assigned to a given resistance mechanism. Resistance profiles of representative healthy individuals and patients with non-small cell lung cancer (NSCLC) displaying clinical benefit (CB) or no CB (NCB) are shown. FDA, US Food and Drug Administration; IND, investigational new drug.

processes: angiogenesis, cell proliferation, chemoresistance, and immune-related processes (figure 7C). We chose to focus the analysis on the pattern D and E RAP subsets under the assumption that they likely contain key drivers of ICI resistance that also represent clinically relevant targets. Indeed, 20% of the pattern D and E RAPs were targets of therapeutic agents, and 21 RAPs were putative biomarkers (figure 7C). Next, resistance profiles for individual patients were generated by scoring each resistance-related process. To this end, the median normalized expression level among the RAPs assigned to a particular resistance-related process was used as the score per process for a given individual. Resistance profiles for

selected individuals from the NCB, CB, and healthy populations are shown in figure 7D and are representative of each population (online supplemental figure S8; based on both the Kolmogorov-Smirnov test and Student's t-test; online supplemental table S13A,B). As expected, NCB patients generally had the highest scores. Notably, the resistance profiles varied among the patients; some displayed high scores across several resistance-related processes, whereas others scored high in a single process. These findings highlight the personalized and multilayered nature of treatment resistance. They also suggest that RAP profiles have the potential to personalize treatments by guiding the choice of an add-on treatment to

enhance ICI efficacy in patients at risk of poor outcomes from standard ICI-based therapies.

DISCUSSION

Although ICI-based therapies have advanced cancer care and have improved survival rates in many clinical settings, their efficacy remains suboptimal. Furthermore, ICI toxicity may be substantial in certain patients. Understanding the mechanisms underlying resistance to ICI-based therapies is critical for developing strategies to improve clinical outcomes. Here, we comprehensively characterized blood-based RAP biomarkers in the PROphet model to better understand the underlying biology of poor clinical outcomes in patients with NSCLC receiving ICI-based therapy. Using bioinformatics approaches, we showed that RAPs are associated with various tumor-supporting processes, such as immune modulation, proliferative signaling, ECM, invasion, and metastasis. Furthermore, hierarchical clustering based on RAP expression in a large cohort of 272 patients with NSCLC and 50 healthy subjects identified five distinct RAP subsets, from which further biological and clinical insights could be gained. Specifically, patterns D and E RAPs likely represent critical drivers of ICI resistance and clinically relevant drug targets based on their upregulation in the NCB population and known tumor-promoting roles.

Exploration of the cellular origin of RAPs has revealed interesting trends. RAP characterization based on the HPA and CPTAC databases suggests that these proteins may originate from cancer or the host. This highlights one of the advantages of plasma proteomics, where multiple biomarkers originating from different cell types are more likely to capture the interplay between the tumor, its microenvironment, and systemic processes. Specifically, this analysis showed that the RAP set was enriched with lung cancer-related and liver-related proteins. The lung cancer-related RAPs displayed significant enrichment of various cancer hallmarks and tumor factors associated with poor prognosis, suggesting that some RAPs reflect tumor-intrinsic properties.

Moreover, such RAPs may represent novel targets for intervention or serve as plasma-based biomarkers for tumor status. Regarding liver-related RAPs, our findings show that their enrichment is not associated with liver metastasis but may reflect a broader involvement of liver function in determining clinical outcomes. Possible explanations include drug metabolism and systemic liver-mediated immune response or tolerance.[44] Indeed, IL-6 signaling in hepatocytes has been shown to regulate T-cell surveillance in extrahepatic tumors.[45] This aligns with our findings, suggesting a hepatocyte origin for liver-related RAPs and high expression of IL-6 in NCB patients. It would be interesting to investigate whether liver-related RAPs can serve as predictive biomarkers for the development of hepatic immune-related adverse

events during ICI therapy. Notably, we provide two lines of evidence suggesting a relationship between RAPs and the liver: (1) enrichment of liver-associated proteins among RAPs and (2) enrichment of RAPs among the liver metastasis-related proteins. The latter includes proteins such as SPINT1, EPHA10, EPHB4, and HAVCR1 that are associated with immunosuppressive immune cells, aligning with previous studies demonstrating an association between liver metastasis and an immune suppressive phenotype.[46] The connection between liver, clinical benefit and RAPs should be further explored in a follow-up study, potentially addressing liver-related mechanisms for resistance to treatment.

In line with the mechanism of action of ICIs, approximately one-third of all RAPs were categorized as potentially originating from immune cells. The current study demonstrates a relationship between RAPs and distinct immune-related processes. For example, tumor-promoting inflammation was enriched in core RAPs, whereas acute-phase response and complement system proteins were enriched in the liver-related RAP set. Although acute phase response proteins are considered non-specific inflammatory markers, various studies have demonstrated their prognostic and predictive value in patients with cancer.[36 47] The complement system, an essential component of innate immunity, has emerged as a significant regulator of cancer immunity, with an established role in promoting an immunosuppressive tumor microenvironment.[37] Interestingly, it has been shown that hepatocyte-mediated complement synthesis and secretion are elevated in patients with lung cancer, possibly because of stress-induced secretory products derived from lung cancer tissue.[48] Notably, pattern E RAPs include multiple proteins with immunomodulatory functions. Of particular relevance is IL-6, which has been extensively studied in the context of resistance to ICIs.[49-51] In the functional network of pattern E RAPs, IL-6 was situated at the hub of a cluster of immune-related RAPs, further highlighting its biological relevance. SERPINA1, which encodes alfa1-antitrypsin, is another protein of interest given its recognized role in the acute-phase response and its association with cancer and poor prognosis.[52] Furthermore, multiple proteins implicated in immune checkpoint signaling were found among pattern D and E RAPs. These include FGL-1, which serves as a ligand of the LAG3 immune checkpoint protein[40]; TIM-1 (encoded by HAVCR1), proposed to act as a B cell-specific checkpoint protein that regulates antitumor immunity[53]; and CD39 (encoded by ENTPD1), associated with T cell exhaustion.[54] Notably, biological pathways related to adaptive immunity were not enriched in the RAP set or subsets analyzed in this study. One explanation is that RAPs indicate pretreatment states characterized by various biological processes. This contrasts with on-treatment biomarkers that reflect ICI-induced effects, presumably generating a more prominent signal for adaptive immune processes. Indeed, our previous study investigating on-treatment plasma

proteomic changes reported a strong induction of T cell-mediated processes during ICI treatment.[8]

RAPs prominently represented various additional processes associated with treatment resistance: (1) The "invasion and metastasis" category was enriched in the entire RAP set and several RAP subsets, suggesting that many RAPs serve as indicators of aggressive disease. This has clinical implications considering the current treatment guidelines for patients with NSCLC. Specifically, for patients with a PD-L1 TPS≥50%, adding chemotherapy to ICIs is recommended in cases of aggressive disease.[4] Indeed, among patients with PD-L1 TPS≥50%, the model identifies cases in which ICI-chemotherapy combination is preferable over ICI monotherapy,[11] suggesting an ability to detect aggressive disease based solely on proteomic profiles. (2) ECM-related proteins were highly represented among the RAPs. This aligns with emerging evidence demonstrating that ECM is a critical component that affects ICI efficacy. Specifically, tumor-associated ECM contributes to a pro-tumoral environment by educating tumor microenvironment cells to promote tumor progression. In addition, a highly dense and stiff ECM creates a physical barrier to immune cell infiltration, thus protecting the tumor from immune-mediated destruction.[55] (3) The RAP set consisted of multiple splicing-related proteins associated with ICI resistance. For example, RBFOX2 promotes alternative splicing that drives epithelial-mesenchymal transition and tissue invasiveness,[56] whereas PUF60 supports lung cancer progression via alternative splicing of the cell cycle regulator CDC25.[57] Indeed, RNA splicing is frequently dysregulated in various cancer types and has been shown to correlate with immunosuppression and unfavorable outcomes in ICI-treated cancers.[58]

From a clinical perspective, we explored the potential of RAPs to aid in the future development of personalized therapies. We envision several possibilities in which RAPs can guide treatment choices to enhance the therapeutic effects of ICIs. First, individual RAPs could be targeted by ICIs in patients at risk for poor outcomes from standard ICI-based therapies, particularly those with elevated circulating levels of these RAPs. Several ongoing trials have evaluated these combinations. For example, agents that inhibit pattern D and E RAPs, CD39, EPHB4, and IL-6 are under investigation in combination with ICIs for various cancers (NCT04261075, NCT03884556, NCT03049618, NCT04691817, and NCT04940299). Therefore, RAP profiles could potentially match patients to appropriate clinical trials prospectively. Second, patient resistance profiles might help to identify an appropriate drug class or treatment modality for combination with ICIs. For example, patients scoring high in the angiogenesis category might benefit from the addition of antiangiogenic agents to the treatment plan. In contrast, those with a high cell proliferation score may be appropriate candidates for the addition of chemotherapy or radiotherapy. Third, patient resistance profiles might help to identify the most suitable choice among the available RAP-targeting drugs. Specifically, RAPs from high-scoring resistance-related processes may be more appropriate targets for individual patients than those from low-scoring ones. Clinical trials assessing specific drug combinations in patient populations with varied RAP profiles are necessary to determine the clinical value of these theoretical approaches.

A potential limitation of this study is that RAPs were initially identified using pretreatment blood samples. Thus, whether they reflect primary or acquired resistance remains to be determined. Therefore, preclinical and clinical studies are needed to address this question. Another potential limitation is the inclusion of a mixed cohort of patients with NSCLC receiving either ICI treatment alone or in combination with chemotherapy. As a result, some RAPs might be linked to chemotherapy rather than immunotherapy.

Overall, our study provides a biological rationale for the predictive ability of the PROphet model in the context of NSCLC. Furthermore, it highlights the potential clinical value of RAPs for developing personalized therapies that address resistance to ICI-based treatment.

Author affiliations

[1]OncoHost Ltd, Binyamina, Israel

[2]Department of Medicine, Roswell Park Comprehensive Cancer Center, Buffalo, New York, USA

[3]The Roswell Park Comprehensive Cancer Center Data Bank and BioRepository, Buffalo, New York, USA

[4]Department of Hematology and Oncology, Baylor University Medical Center at Dallas, Dallas, Texas, USA

[5]Faculty of Medicine, Technion Israel Institute of Technology, Haifa, Israel

[6]Shamir Medical Center, Zerifin, Israel

[7]The Ohio State University, Columbus, Ohio, USA

[8]Division of Hematology/Oncology, UC Davis Comprehensive Cancer Center, Sacramento, California, USA

[9]Sidney Kimmel Medical College, Thomas Jefferson University, Philadelphia, Pennsylvania, USA

ORCID iDs
Michal Harel http://orcid.org/0000-0002-6384-1523
Coren Lahav http://orcid.org/0000-0003-4497-9348
Igor Puzanov http://orcid.org/0000-0002-9803-3497
Yuval Shaked http://orcid.org/0000-0001-9037-3895
David P Carbone http://orcid.org/0000-0003-3002-1921
David R Gandara http://orcid.org/0000-0003-1784-048X

REFERENCES

1 Pardoll DM. The blockade of immune checkpoints in cancer immunotherapy. *Nat Rev Cancer* 2012;12:252–64.
2 Bagchi S, Yuan R, Engleman EG. Immune Checkpoint Inhibitors for the Treatment of Cancer: Clinical Impact and Mechanisms of Response and Resistance. *Annu Rev Pathol* 2021;16:223–49.
3 Gibney GT, Weiner LM, Atkins MB. Predictive biomarkers for checkpoint inhibitor-based immunotherapy. *Lancet Oncol* 2016;17:e542–51.
4 Jaiyesimi IA, Leighl NB, Ismaila N, *et al*. Therapy for Stage IV Non-Small Cell Lung Cancer Without Driver Alterations: ASCO Living Guideline, Version 2023.3. *J Clin Oncol* 2024;42:e23–43.
5 Waterhouse D, Lam J, Betts KA, *et al*. Real-world outcomes of immunotherapy-based regimens in first-line advanced non-small cell lung cancer. *Lung Cancer (Auckl)* 2021;156:41–9.
6 Cancer immunotherapy: the quest for better biomarkers. *Nat Med* 2022;28:2437.
7 Marabelle A, Fakih M, Lopez J, *et al*. Association of tumour mutational burden with outcomes in patients with advanced solid tumours treated with pembrolizumab: prospective biomarker analysis of the multicohort, open-label, phase 2 KEYNOTE-158 study. *Lancet Oncol* 2020;21:1353–65.
8 Bar J, Leibowitz R, Reinmuth N, *et al*. Biological insights from plasma proteomics of non-small cell lung cancer patients treated with immunotherapy. *Front Immunol* 2024;15:1364473.
9 Harel M, Lahav C, Jacob E, *et al*. Longitudinal plasma proteomic profiling of patients with non-small cell lung cancer undergoing immune checkpoint blockade. *J Immunother Cancer* 2022;10:e004582.
10 Yellin B, Lahav C, Sela I, *et al*. Analytical validation of the PROphet test for treatment decision-making guidance in metastatic non-small cell lung cancer. *J Pharm Biomed Anal* 2024;238:115803.
11 Christopoulos P, Harel M, McGregor K, *et al*. Plasma Proteome-Based Test for First-Line Treatment Selection in Metastatic Non-Small Cell Lung Cancer. *JCO Precis Oncol* 2024;8:e2300555.
12 Gold L, Ayers D, Bertino J, *et al*. Aptamer-based multiplexed proteomic technology for biomarker discovery. *PLoS One* 2010;5:e15004.
13 Tyanova S, Temu T, Sinitcyn P, *et al*. The Perseus computational platform for comprehensive analysis of (prote)omics data. *Nat Methods* 2016;13:731–40.
14 Szklarczyk D, Gable AL, Nastou KC, *et al*. The STRING database in 2021: customizable protein-protein networks, and functional characterization of user-uploaded gene/measurement sets. *Nucleic Acids Res* 2021;49:D605–12.
15 Liebermeister W, Noor E, Flamholz A, *et al*. Visual account of protein investment in cellular functions. *Proc Natl Acad Sci U S A* 2014;111:8488–93.
16 Lever J, Jones MR, Danos AM, *et al*. Text-mining clinically relevant cancer biomarkers for curation into the CIViC database. *Genome Med* 2019;11:78.
17 Cannon M, Stevenson J, Stahl K, *et al*. DGIdb 5.0: rebuilding the drug-gene interaction database for precision medicine and drug discovery platforms. *Nucleic Acids Res* 2024;52:D1227–35.
18 Hermeking H. The 14-3-3 cancer connection. *Nat Rev Cancer* 2003;3:931–43.
19 Skoulidis F, Araujo HA, Do MT, *et al*. CTLA4 blockade abrogates KEAP1/STK11-related resistance to PD-(L)1 inhibitors. *Nature New Biol* 2024;635:462–71.
20 Indini A, Rijavec E, Ghidini M, *et al*. Impact of BMI on Survival Outcomes of Immunotherapy in Solid Tumors: A Systematic Review. *Int J Mol Sci* 2021;22:2628.
21 Sung M, Jang WS, Kim HR, *et al*. Prognostic value of baseline and early treatment response of neutrophil-lymphocyte ratio, C-reactive protein, and lactate dehydrogenase in non-small cell lung cancer patients undergoing immunotherapy. *Transl Lung Cancer Res* 2023;12:1506–16.
22 Davies MPA, Sato T, Ashoor H, *et al*. Plasma protein biomarkers for early prediction of lung cancer. *EBioMedicine* 2023;93:104686.
23 Yuan X, Duan Y, Xiao Y, *et al*. Vitamin E Enhances Cancer Immunotherapy by Reinvigorating Dendritic Cells via Targeting Checkpoint SHP1. *Cancer Discov* 2022;12:1742–59.
24 Yang Z, Feng J, Xiao L, *et al*. Tumor-Derived Peptidoglycan Recognition Protein 2 Predicts Survival and Antitumor Immune Responses in Hepatocellular Carcinoma. *Hepatology* 2020;71:1626–42.
25 Considine RV, Sinha MK, Heiman ML, *et al*. Serum immunoreactive-leptin concentrations in normal-weight and obese humans. *N Engl J Med* 1996;334:292–5.
26 Dudzinski SO, Bader JE, Beckermann KE, *et al*. Leptin Augments Antitumor Immunity in Obesity by Repolarizing Tumor-Associated Macrophages. *J Immunol* 2021;207:3122–30.
27 Li Z-C, Wang J, Liu H-B, *et al*. Proteomic and metabolomic features in patients with HCC responding to lenvatinib and anti-PD1 therapy. *Cell Rep* 2024;43:113877.
28 Mahmood N, Rabbani SA. DNA Methylation Readers and Cancer: Mechanistic and Therapeutic Applications. *Front Oncol* 2019;9:489.

29 Gogesch P, Dudek S, van Zandbergen G, *et al*. The Role of Fc Receptors on the Effectiveness of Therapeutic Monoclonal Antibodies. *Int J Mol Sci* 2021;22:8947.

30 Guo S, Han F, Zhu W. CD39 - A bright target for cancer immunotherapy. *Biomed Pharmacother* 2022;151:113066.

31 Daly RJ, Scott AM, Klein O, *et al*. Enhancing therapeutic anti-cancer responses by combining immune checkpoint and tyrosine kinase inhibition. *Mol Cancer* 2022;21:189.

32 Zhang J, Liu G, Liu Y, *et al*. The biological functions and related signaling pathways of SPON2. *Front Oncol* 2023;13:1323744.

33 Li Q, Wei K, Zhang X, *et al*. TIMP1 shapes an immunosuppressive microenvironment by regulating anoikis to promote the progression of clear cell renal cell carcinoma. *Aging (Milano)* 2023;15:8908–29.

34 Deng K, Yao J, Huang J, *et al*. Abnormal alternative splicing promotes tumor resistance in targeted therapy and immunotherapy. *Transl Oncol* 2021;14:101077.

35 Saad HM, Tourky GF, Al-Kuraishy HM, *et al*. The Potential Role of MUC16 (CA125) Biomarker in Lung Cancer: A Magic Biomarker but with Adversity. *Diagnostics (Basel)* 2022;12:2985.

36 Schneider MA, Rozy A, Wrenger S, *et al*. Acute Phase Proteins as Early Predictors for Immunotherapy Response in Advanced NSCLC: An Explorative Study. *Front Oncol* 2022;12:772076.

37 Pio R, Ajona D, Ortiz-Espinosa S, *et al*. Complementing the Cancer-Immunity Cycle. *Front Immunol* 2019;10:774.

38 Klement JD, Paschall AV, Redd PS, *et al*. An osteopontin/CD44 immune checkpoint controls CD8+ T cell activation and tumor immune evasion. *J Clin Invest* 2018;128:5549–60.

39 Li G, Javed M, Rasool R, *et al*. A pan-cancer analysis of HAVCR1 with a focus on diagnostic, prognostic and immunological roles in human cancers. *Am J Transl Res* 2023;15:1590–606.

40 Wang J, Sanmamed MF, Datar I, *et al*. Fibrinogen-like Protein 1 Is a Major Immune Inhibitory Ligand of LAG-3. *Cell* 2019;176:334–47.

41 Eltahir M, Isaksson J, Mattsson JSM, *et al*. Plasma Proteomic Analysis in Non-Small Cell Lung Cancer Patients Treated with PD-1/PD-L1 Blockade. *Cancers (Basel)* 2021;13:3116.

42 Musaelyan AA, Lapin SV, Urtenova MA, *et al*. Inflammatory and autoimmune predictive markers of response to anti-PD-1/PD-L1 therapy in NSCLC and melanoma. *Exp Ther Med* 2022;24:557.

43 Shaked Y. The pro-tumorigenic host response to cancer therapies. *Nat Rev Cancer* 2019;19:667–85.

44 Shojaie L, Ali M, Iorga A, *et al*. Mechanisms of immune checkpoint inhibitor-mediated liver injury. *Acta Pharm Sin B* 2021;11:3727–39.

45 Stone ML, Lee J, Lee JW, *et al*. Hepatocytes coordinate immune evasion in cancer via release of serum amyloid A proteins. *Nat Immunol* 2024;25:755–63.

46 Lee JC, Green MD, Huppert LA, *et al*. The Liver-Immunity Nexus and Cancer Immunotherapy. *Clin Cancer Res* 2022;28:5–12.

47 Naqash AR, McCallen JD, Mi E, *et al*. Increased interleukin-6/C-reactive protein levels are associated with the upregulation of the adenosine pathway and serve as potential markers of therapeutic resistance to immune checkpoint inhibitor-based therapies in non-small cell lung cancer. *J Immunother Cancer* 2023;11:e007310.

48 Zhao P, Wu J, Lu F, *et al*. The imbalance in the complement system and its possible physiological mechanisms in patients with lung cancer. *BMC Cancer* 2019;19:201.

49 Huseni MA, Wang L, Klementowicz JE, *et al*. CD8+ T cell-intrinsic IL-6 signaling promotes resistance to anti-PD-L1 immunotherapy. *Cell Reports Medicine* 2023;4:100878.

50 Khononov I, Jacob E, Fremder E, *et al*. Host response to immune checkpoint inhibitors contributes to tumor aggressiveness. *J Immunother Cancer* 2021;9:e001996.

51 Laino AS, Woods D, Vassallo M, *et al*. Serum interleukin-6 and C-reactive protein are associated with survival in melanoma patients receiving immune checkpoint inhibition. *J Immunother Cancer* 2020;8:e000842.

52 Ercetin E, Richtmann S, Delgado BM, *et al*. Clinical Significance of SERPINA1 Gene and Its Encoded Alpha1-antitrypsin Protein in NSCLC. *Cancers (Basel)* 2019;11:1306.

53 Bod L, Kye Y-C, Shi J, *et al*. B-cell-specific checkpoint molecules that regulate anti-tumour immunity. *Nature New Biol* 2023;619:348–56.

54 Canale FP, Ramello MC, Núñez N, *et al*. CD39 Expression Defines Cell Exhaustion in Tumor-Infiltrating CD8⁺ T Cells. *Cancer Res* 2018;78:115–28.

55 Fejza A, Carobolante G, Poletto E, *et al*. The entanglement of extracellular matrix molecules and immune checkpoint inhibitors in cancer: a systematic review of the literature. *Front Immunol* 2023;14:1270981.

56 Braeutigam C, Rago L, Rolke A, *et al*. The RNA-binding protein Rbfox2: an essential regulator of EMT-driven alternative splicing and a mediator of cellular invasion. *Oncogene* 2014;33:1082–92.

57 Xu N, Ren Y, Bao Y, *et al*. PUF60 promotes cell cycle and lung cancer progression by regulating alternative splicing of CDC25C. *Cell Rep* 2023;42:113041.

58 Chen Z, Chen C, Li L, *et al*. The spliceosome pathway activity correlates with reduced anti-tumor immunity and immunotherapy response, and unfavorable clinical outcomes in pan-cancer. *Comput Struct Biotechnol J* 2021;19:5428–42.